Applied Energy 107 (2013) 89–97

Contents lists available at SciVerse ScienceDirect

Applied Energy

journal homepage: www.elsevier.com/locate/apenergy

Theoretical and experimental investigation on a thermoelectric cooling and heating system driven by solar

Wei He *, Jinzhi Zhou, Jingxin Hou, Chi Chen, Jie Ji

Department of Thermal Science and Energy Engineering, University of Science and Technology of China, Hefei 230026, China

HIGHLIGHTS

- Thermoelectric devices united with PV/T panel can cool rooms, heat water in summer and heat rooms in winter.
- The simulation results in summer have been validated by experiment.
- The system can be applied conveniently and operates quietly.

ARTICLE INFO

Article history:
Received 20 April 2012
Received in revised form 19 September 2012
Accepted 19 January 2013
Available online 6 March 2013

Keywords:
Solar
Thermoelectric cooling and heating systems
PV/T
COP
Thermal efficiency

ABSTRACT

Buildings composited with thermoelectric cooling and heating systems use solar energy to cool rooms in summer and heat rooms in winter via thermoelectric devices and photovoltaic/thermal (PV/T) dual function modules. In summer, the thermoelectric device works as a Peltier cooler when electrical power supplied by PV/T modules is applied on it. The cold side absorbs heat from indoor to decrease the temperature of the room. In the meanwhile, the thermal energy gained both from the hot side and PV/T system is collected to heat domestic water by heat pipes. In winter, the voltage applied on thermoelectric device is reversed with PV/T modules being power and heat source simultaneously to thermoelectric device and then thermoelectric device could release heat to increase the temperature of the room. The experiments has been done in a model room whose volume is 0.125 m^3, in summer condition, using solar panel whose area is 0.5 m^2. The minimum temperature 17 °C is achieved, with COP of the thermoelectric device higher than 0.45. The temperature of water in the storage tank with a volume of 18.5 L has risen about 9 °C. The thermal efficiency of the system is 12.06%. This simple and environmentally friendly can reduce cooling and heating load in room.

1. Introduction

Air-conditioner (AC) has become almost indispensable for every family, but the traditional air-conditioner has some disadvantages as following: (1) Traditional AC systems consume too much energy. To meet their demands, natural resources are burned to generate electricity, which causes greenhouse effect and to exacerbate a lot of pollution on the earth. (2) The refrigerant of traditional air-conditioner, Freon, once leaked, will cause irreversible damage to the ozone sphere and make life suffer from ultraviolet radiation. Hence buildings composited thermoelectric cooling and heating systems are proposed. They use thermoelectric devices for cooling and heating and thus it reduces the utilization of traditional energy source, without doing any harm to the environment.

There are two main applications of thermoelectric. One is electricity generation with waste energy and renewable energy. Rowe DM, Min Gao have evaluated thermoelectric modules for power generation [1]. He et al. have described a solar heat pipe thermoelectric generator (SHP-TEG) unit comprising an evacuated double-skin glass tube, a finned heat pipe and a TEG module [2,3]. Niu, Yu, Gou, Xiao have reported the experimental study on low-temperature waste heat thermoelectric generator [4,5].

Another main application of thermoelectric is for cooling. Nowadays there is much more using space in the area of thermoelectric refrigeration, such as the scientific equipment applications, household application, and computer equipment [6], as it s no needing working fluid and moving part. And the cooling performance of thermoelectric refrigeration has been experimented and simulated by many researchers in different modes [7–10]. But it is not enough to investigate the efficiency of the thermoelectric materials singly [11], the widespread use of thermoelectric refrigeration is that it should be combined with other devices to achieve a much more complex role. The thermoelectric refrigerator has been developed, simulated using computational model, based on the finite difference method [12]. Chen et al. have analyzed the energy efficiency

* Corresponding author.
E-mail address: hwei@ustc.edu.cn (W. He).

0306-2619/$ - see front matter © 2013 Elsevier Ltd. All rights reserved.
http://dx.doi.org/10.1016/j.apenergy.2013.01.055

Nomenclature

Q	heat flow (W)
α	absorptivity or Seebeck coefficient thermoelectric materials (V/K)
U	voltage (V)
I	current (A)
T	temperature (°C)
L	thickness (m)
σ	conductivity of the thermoelectric materials ($1/\rho$)
S	area (m^2)
K	thermal conductivity (W/m K)
A	contact area (m^2)
R	thermal resistance (K/W)
R'	thermal contact resistance (K/W)
R''	contact resistance coefficient (m^2K/W)
Y	perimeter of radiator (m)
u	speed of wind (m/s)
b	length of radiator (m)
P	power (W)
r	radius of heat pipe m
d	width of copper (m)
C_p	heat capacity (kJ/(kg k))
M	quality (kg)
ΔT	temperature variation of water (°C)
W_{solar}	solar irradiance (W/m^2)
η_e	electrical efficiency of the system
η_{pump}	efficiency of the pump
η_t	thermal efficiency of the system
η_{pv}	theory electrical efficiency of solar cells
n	number
τ	interval time of data collection

Subscripts

1	ceramic shell of thermoelectric device
2	copper plate
3	heat pipe
4	the heat exchanger
5	the storage tank
6	circulation line
7	the radiator
8	the experimental room
c	cold side of a thermoelectric module
h	hot side of a thermoelectric module
r	the experimental room
t	thermoelement
s	thermoelectric device
fin	fin of the radiator
evn	environment
fan	fan
pipe	heat pipe
w_1	water in the heat exchanger
w_2	water in the storage tank
w_3	water in the experimental room
total	total
pump	pump
solar	solar cell
tank	storage tank
air	air in the experimental room
heat-rc	cold side of thermoelectric device and experimental room
heat-re	environment and experimental room
heat-cp	thermoelectric device and heat pipe
heat-ip	heat pipe and heat exchanger
loss-i.e.	heat exchanger and environment
loss-te	storage tank and environment
loss-ce	circulation line and environment

of thermoelectric power cycle to today's CHP systems and its impact on the application [13]. Chen et al. have studied a model of thermoelectric generator-driven thermoelectric refrigerator with external heat transfer [14]. It described how to allocate heat transfer surface area of four heat exchangers to maximize the cooling load and the coefficient of performance (COP) of the combined thermoelectric refrigerator device. And they also have reported the extreme working temperature differences of combined thermoelectric devices, using non-equilibrium thermodynamics [15] and the performance prediction and irreversibility analysis of a thermoelectric refrigerator with finned heat exchanger [16].

The research of thermoelectric device combined with the solar energy is expanding [17]. The solar energy is convenient, environmental protection and inexhaustible. Solar energy collection technology has been applied to certain extent, but solar cooling technique has not been well developed. Currently, the main technologies in the area of solar air-conditioning in building are solar absorption cooling, solar jet cooling, solar liquid-descanting cooling, and solar-driven thermoelectric cooling. In the past years, a lot of work has been reported on thermoelectric cooling. Dai et al. undertook the research on a thermoelectric device driven by solar cells [18]. Van Sark reported the performance of the thermoelectric hybrid modules [19]. Hara researched a solar cell driven thermoelectric cooling prototype headgear for outside personal cooling [20]. Atta studied solar water condensation by using thermoelectric coolers [21]. Their research on solar thermoelectric cooling has provided a wealth of valuable data and analysis.

The main significance of this design of this paper is to study the building integrated solar photovoltaic/thermal (BIPV/T) technology in the application of low-carbon buildings. Compared with the thermoelectric refrigerator, the system can cool the room with cooling mode of thermoelectric powered by PV/T modules, get hot water using heat pipes and PV/T modules in summer, and in winter, heat the room with heating mode of thermoelectric, PV/T modules being power and heat source simultaneously. The energy-saving system is acoustically silent and environmentally friendly. Thus, it can be applied in a vast area.

2. The system working principle

The following diagram (Fig. 1) shows the system's working structure in summer. The bottom of a heat pipe (1) is welded on the back of solar cells, while the top is inserted in the heat exchanger. The bottom of thermoelectric device in the experimental room is connected to radiator whose material is aluminum, and the top is connected to the evaporator end of heat pipe (2) whose condenser end is inserted into the outside heat exchanger. On one hand, the photovoltaic/thermal (PV/T) system transports the heat gotten from the sunlight into the heat exchanger through heat pipes (1); on the other hand, when the thermoelectric device is powered by PV/T system, its cold side absorbs heat and the hot side releases a lot of heat which will be transported into the heat exchanger by heat pipe (2). And the heat exchanger is linked to a

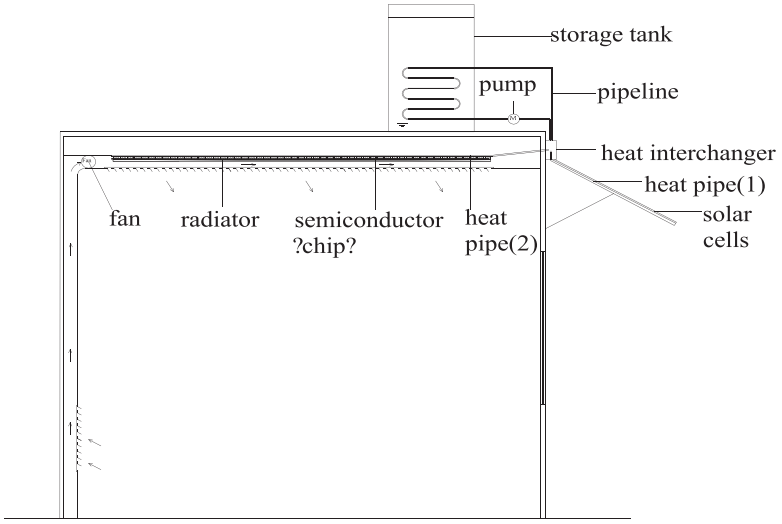

Fig. 1. The working principle of the system in summer.

storage tank through a circulating pump which can transport heat between them. The fan and radiator which are tied to the cold side will discharge cold more efficiently, which causes the temperature of experimental room drop quickly.

3. Mathematical models

Many tests have been taken on the performance of heat pipe PV/T system. Pei et al. [22] have investigated the simulation and experimental study on the heat pipe PV/T system. He et al. [23] have reported the study of comparative experiment on photovoltaic and thermal solar system. Both of them have done a specific analysis on its electrical efficiency and thermal efficiency. Therefore we only use a single solar cell to test the capacity of the thermoelectric device in this experiment.

The system consists of solar cells, experimental room which is installed with thermoelectric device, heat exchanger and storage tank. As shown in Fig. 2.

The experimental room is combined with foam box whose volume is 0.125 m^3, thermoelectric devices, radiators and heat pipes. The cold side of thermoelectric device is bonded to the radiator tightly by silicon grease, and the hot side is bonded to a copper plate by silicon grease which can enhance heat transfer. There is a groove whose shape is as the same as the heat pipe on the other side of copper plate. The evaporator end of heat pipe is embedded into the groove to enlarge the contact area, and the condenser end is inserted into the heat exchanger, thus, the heat can spread into the water quickly. The heat exchanger is connected to the storage tank by a circulating pump that can transfer heat quickly between them.

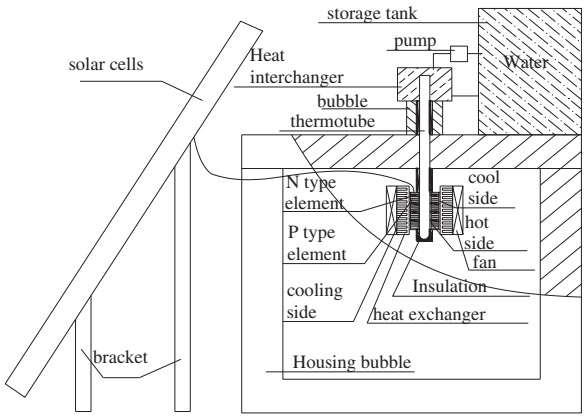

Fig. 2. Experimental investigation and simulation on a thermoelectric cooling and heating system driven by solar.

3.1. The cold and hot side of the thermoelectric device

3.1.1. The heat balance of the cold side of thermoelectric device may be given by [24]:

$$Q_C = n_t\left[\alpha I_t T_c - \frac{I_t^2 L_t}{\sigma S_t} - \frac{2S_t K_t (T_h - T_c)}{L_t}\right] \tag{1}$$

3.1.2. The heat balance equation of the hot side [24]:

$$Q_h = n_t\left[\alpha I_t T_h + \frac{I_t^2 L_t}{\sigma S_t} - \frac{2S_t K_t (T_h - T_c)}{L_t}\right] \tag{2}$$

where Q_c is the heat absorption of cold side of thermoelectric device, Q_h is the heat that the hot side of thermoelectric device has released, α is the Seebeck coefficient of thermoelectric materials (p-type and n-type assumed to be same), I_t is the current. S_t and L_t are the cross-section area and length of thermoelement, respectively, σ and K_t are the conductivity and thermal conductivity of the thermoelectric materials, n_t is the number of thermoelements, T_c and T_h are the temperature of cold side and hot side of thermoelectric device.

3.2. The experimental room

3.2.1. The heat balance between the cold side of thermoelectric device and experimental room is expressed as:

$$Q_{heat\text{-}rc} = \frac{T_c - T_r}{R_1 + R'_{17} + R_7} \tag{3}$$

where $Q_{heat\text{-}rc}$ is the heat transfer between the cold side of thermoelectric device and the experimental room, and T_r is the temperature of the experimental room. R_1 is the thermal resistance of ceramic shell of thermoelectric device, given by:

$$R_1 = \frac{L_1}{K_1 S_1} \tag{4}$$

where L_1 is the thickness of ceramic, K_1 is the thermal conductivity of the ceramics, S_1 is the area of ceramic. In this case, L_1 is 0.5 mm, K_1 equals to 3.98 W/(m K), S_1 is16 cm.

R'_{17} is the thermal contact resistance between the thermoelectric device and radiator, expressed as:

$$R'_{17} = \frac{R''_{17}}{A_{17}} \tag{5}$$

where R''_{17} is the thermal contact resistance coefficient between the ceramics and aluminum which is 4×10^{-5}m^2 K/W, A_{17} is the contact area which is 16 cm^2.

R_7 is the thermal resistance of the radiator, calculated by the following equation [25]:

$$R_7 = \frac{1}{1.16K_7L_7bn_{fin}} + \frac{1 - 0.152(ub)^{-\frac{1}{10}}}{5.12u^{\frac{4}{5}}Y} \tag{6}$$

where b is the length of radiator, Y is the perimeter of radiator, L_7 is the thickness of fin, n_{fin} is the number of the fins, u is the speed of wind, K_7 is the thermal conductivity of the aluminum which is 240 W/(m K).

3.2.2. The heat balance between the environment and experimental room may be calculated by the following equation:

$$Q_{heat\text{-}re} = K_8S_8\frac{(T_{env} - T_r)}{L_8} \tag{7}$$

where $Q_{heat\text{-}re}$ is the heat transferred between the environment and experimental room, K_8 is the thermal conductivity of the foam board which is 0.05 W/(m K), T_{evn} is the temperature of environment, S_8 is the area of foam board which is 1.5 m^2, L_8 is the thickness of foam board which is 15 cm.

3.2.3. The equation of fan is provided by:

$$P_{fan} = U_{fan}I_{fan} \tag{8}$$

where P_{fan} is the power of fan, U_{fan} is the voltage of fan, I_{fan} stands for the current.

3.3. The heat balance between the thermoelectric device and heat pipe is expressed as

$$Q_{heat\text{-}cp} = \frac{T_h - T_{pipe}}{R_1 + R_2 + R_3 + R'_{12} + R'_{23}} \tag{9}$$

where $Q_{heat\text{-}cp}$ is the heat s transfer between the thermoelectric device and heat pipes, T_{pipe} is the temperature of heat pipe.

R_2 is the thermal resistance of copper with a groove, given by:

$$R_2 = \frac{L_2}{\pi rdK_2} \tag{10}$$

R_3 is the thermal resistance of wall of heat pipe, expressed as:

$$R_3 = \frac{L_3}{\pi rdK_2} \tag{11}$$

where L_2 is the thickness of copper which is 3 mm, L_3 is the thickness of wall of heat pipe which is 0.5 mm, r is radius of heat pipe which is 4 mm, d is the width of copper plate which is 4 cm, K_2 is the thermal conductivity of copper which is 400 W/(m K).

R'_{12} is the contact resistance between the ceramic and copper, given by:

$$R'_{12} = \frac{R''_{12}}{A_{12}} \tag{12}$$

R'_{23} is the contact resistance between the copper and heat pipe, expressed as:

$$R'_{23} = \frac{R''_{23}}{A_{23}} \tag{13}$$

where R''_{12} is the contact resistance coefficient ceramic and copper which is 3×10^{-5}m^2 K/W, A_{12} is the contact area which is 16 cm^2, R''_{23} is the contact resistance coefficient between copper and heat pipes which is 2×10^{-5}m^2 K/W, A_{23} is the contact area which is 10 cm^2.

3.4. The heat exchanger

3.4.1. The heat balance between heat pipe and heat exchanger can be calculated by:

$$Q_{heat\text{-}ip} = K_2S_3\frac{T_{pipe} - T_{w1}}{L_3} \tag{14}$$

where $Q_{heat\text{-}ip}$ is the heat transfer between the heat pipe and heat exchanger, S_3 is the contact area between wall and water which is 20 cm^2, T_{w1} is the temperature of the water in heat exchanger.

3.4.2. The heat balance between the heat exchanger and environment may be given by:

$$Q_{loss\text{-}ie} = K_4S_4\frac{T_{w1} - T_{env}}{L_4} \tag{15}$$

where $Q_{loss\text{-}ie}$ is the heat transfer between the heat exchanger and environment, K_4 is the heat transfer coefficient of insulation material which is 0.03 W/km, S_4 is the area of heat exchanger which is 0.06 m^2, L_4 is the thickness of insulation which is 1.5 cm.

3.5. The storage tank

3.5.1. The heat balance of the storage tank is calculated by:

$$Q_{tank} = C_{pw}M_{w2}\Delta T \tag{16}$$

where Q_{tank} is the heat that the water in storage tank has gained, C_{pw} is the specific heat capacity of water which is 4200 kJ/(kg k), M_{w2} stands for the quality of water in storage tank, ΔT denotes the temperature variation of water.

3.5.2. The heat balance between the storage tank and environment is calculated by:

$$Q_{loss\text{-}te} = K_4S_5\frac{T_{W2} - T_{env}}{L_4} \tag{17}$$

where $Q_{loss\text{-}te}$ is the heat transfer between the storage tank and environment, S_5 is the area of storage tank, which is 0.42 m^2, T_{w2} is the temperature of water in a storage tank.

3.6. The circulation line

The heat balance between the circulation line and environment may be given by:

$$Q_{loss\text{-}ce} = K_4S_6\frac{T_{w2} - T_{env}}{L_4} \tag{18}$$

where $Q_{loss\text{-}ce}$ is the heat which is transferred between the circulation line and environment, and S_6 is the area of circulation line, which is 0.06 m^2.

3.7. The Circulating pump

The power of the circulating pump is given by:

$$P_{pump} = U_{pump}I_{pump}\eta_{pump} \tag{19}$$

where P_{pump} is the power of fan, U_{pump} is the voltage of circulating pump, I_{pump} stands for the current, η_{pump} is the efficiency of the pump, which is 0.65.

3.8. Solar cells

The output power is calculated by the following equation [26]:

$$P_{solar} = \eta_{T_{ref}} S_{solar} G_T [1 - 0.0045(T_{solar} - 298.15)] \quad (20)$$

where P_{solar} is the power the PV has output, $\eta_{T_{ref}}$ is the module's electrical efficiency at the reference temperature which is 0.14, S_{solar} is the area of solar array to receive solar irradiation, G_T is the solar radiation flux (irradiance) on module plane, T_{solar} is the module operating temperature.

3.9. Electrical efficiency of the system

$$\eta_e = \frac{n_s U_t I_t}{P_{solar}} \quad (21)$$

where η_e is the electrical efficiency of the solar panel, U_t is the voltage of the thermoelectric device, I_t is the current.

3.10. Coefficient of performance (COP) of the thermoelectric device

$$COP = \frac{Q_c}{U_t I_t} \quad (22)$$

3.11. The thermal efficiency of the system

$$\eta_t = \frac{Q_{tank}}{P_{solar}} \quad (23)$$

Where η_t is the thermal efficiency of the system, Q_{tank} is the heat that the water in storage tank has gained.

3.12. The system

The current of the thermoelectric device:

$$I_t = \sqrt{\frac{P_{solar}\sigma S_t}{2 n_s n_t L_t}} \quad (24)$$

The temperature change of experimental room:

$$\frac{d_{T_r}}{d\tau} = \frac{\tau(n_s Q_c - n_{fan} U_{fan} I_{fan} - K_{er}(T_{env} - T_r))}{C_{pw} M_{w3} + C_{pair} M_{air}} \quad (25)$$

The temperature of cold side of thermoelectric device:

$$T_c = T_r - K_{ec} n_s Q_c \quad (26)$$

The temperature of hot side of thermoelectric device:

$$T_h = n_s Q_h R_{total} + T_{w2} \quad (27)$$

The temperature change of water in storage tank:

$$\frac{dT_w}{d\tau} = \frac{\tau(n_s Q_h - Q_{loss})}{C_{pw} M_{w2}} \quad (28)$$

where K_{er} is the thermal conductivity between the environment and experimental room, K_{ec} is the thermal conductivity between the cold side of thermoelectric device and experimental room. n_s is the number of the thermoelectric devices, τ means the interval time of data collection, n_f is the number of fans, M_{w2} stands for the quality of water in storage tank, M_{w3} is the quality of water in experimental room, C_{pair} is the heat capacity of air, which is 1.01 kj/(kg k), M_{air} is the quality of air in experimental room, R_{total} represents the total thermal resistance between the hot side of thermoelectric device and storage tank, Q_{loss} indicates the total heat loss of storage tank, heat exchanger and circulation line. And the simulation flow chart of this system is shown in Fig. 3.

4. Experimental set-up

The test uses two thermoelectric devices which are connected to solar cell in parallel, and its parameters are listed in the table below (1) (see Table 1):

The model of thermoelectric device used in the test is 127-03 whose rated voltage is 12 V and rated current is 3 A. Three ordinary gravity-type heat pipes are used within the experiment. The radiator and fan are that used on the CPU of desktop computer. The rated voltage of pumps is 12 V and rated current is 2 A. The volume of storage tank is 18.5 L. The experiment set-up is shown in Figs. 4–7.

5. Measurement

The parameters to be recorded in the experiment include solar irradiance, voltage and current of thermoelectric device, the temperature of the cold side and hot side and the temperature of water in storage tank. Some pure water is placed (600 ml) in the experimental room in order to increase heat loss. And a data logger which supplies nine channels to record data is shown in Fig. 4, with the ability to measure voltage directly, current by current sensor and temperature by thermal couples. Channel A records the current of thermoelectric device by using current sensor, channel B is left for recording the voltage directly, channel C measures the temperature of hot side by connecting to thermocouples, channel D measures temperature of cold side, channel E is left for the temperature of pure water in experimental room, channel F is used to record the temperature of experimental room, channel G is left for recording the ambient temperature, channel H records the temperature of water in storage tank, and channel I is used to measure the solar radiation by a pyranometer.

6. Results and analysis

The Fig. 8 shows the variations of output power and solar irradiance in a sunny day. Since not using the controller, the output power and solar irradiance have the same trend in a parabolic shape. And after the calculation, the electrical efficiency of the system is 10.27%.

As shown in Fig. 9, with the solar irradiance increasing and decreasing, the temperature of hot side rises at first and then declines. It is because that the temperature of the hot side is related to the amount of released heat. When irradiation intensity increases in the morning, the output power goes up, causing heat release of the hot side to increase and the temperature to rise. When irradiation intensity appears weak in the afternoon, the output power reduces, leading to the reduction of heat release at the hot side and temperature falling down.

The temperature of experimental room falls to the lowest 17 °C at first and then rises gradually. It can be explained in the following reasons: on the one hand, with temperature gap between the environment and experimental room increasing, the heat transferred between them raises, on the other hand, as the temperature of hot side increasing, the differences in temperature between the cold and hot side increases, which leads the heat transported from the hot side to increase (shown in Fig. 9). In the meanwhile, although the voltage and current of thermoelectric device are increasing, the heat absorption of the cold side is not enough to keep the temperature dropping, resulting in the slow ascent of it.

And as it is shown in the Fig. 10, with the heat absorption decreasing slowly, the COP falls to about 0.45 and then rises gradually. The reason is that while Q_c has hardly changed, the power supplied by solar cells is changing in a parabolic shape. Hence COP behaves in accord with it.

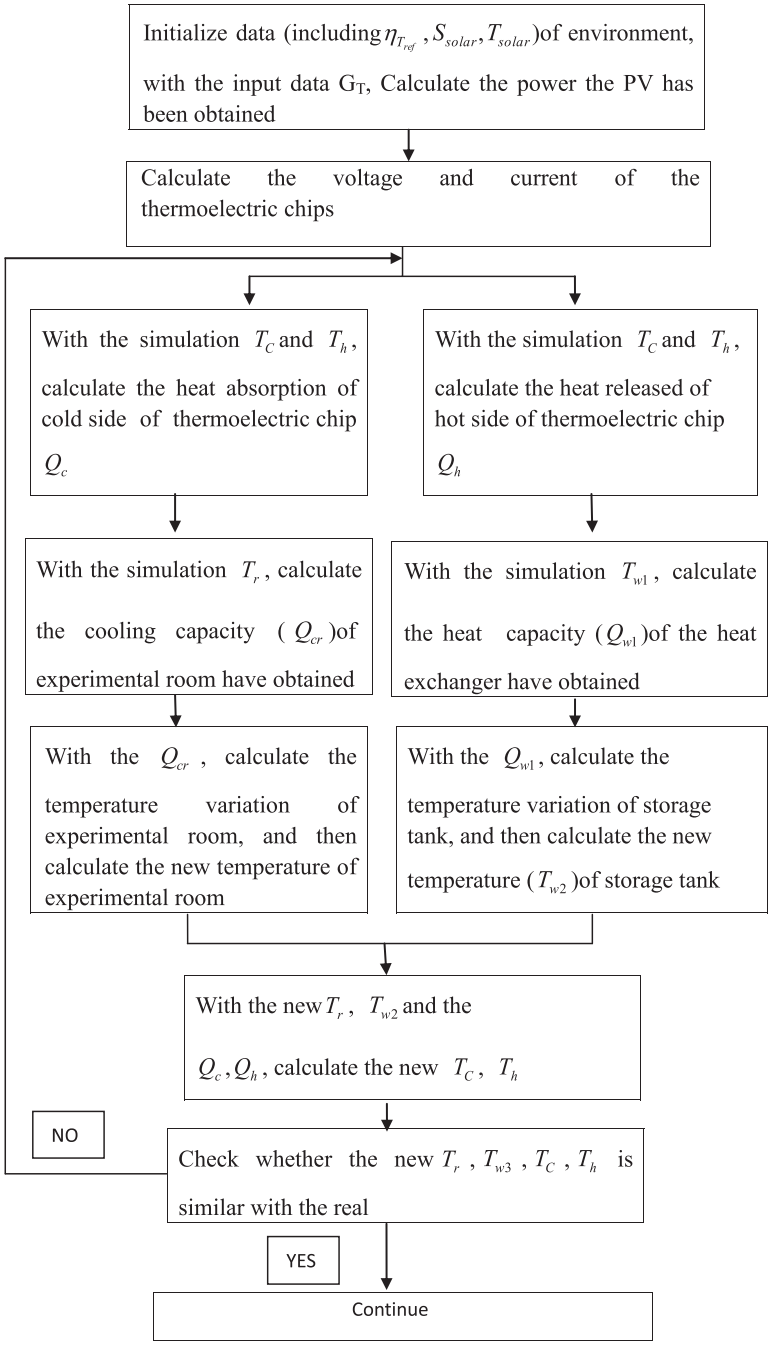

Fig. 3. The simulation flow chart.

Table 1
The parameters of the solar cell thermoelectric chip and heat pipe.

Solar panel	Thermoelectric device		Heat pipe	
Area 0.5 m^2	Z	2.8–3.0 × 10^{-3}	Length	0.35 m
	α	2.1 × 10^3 (V/K)	Diameter	0.008 m
	K	160–180(W/k m)	The thickness of wall	5 × 10^{-4} m
	σ	1.0 × 10^5 (1/Ω m)		
	γ	14.13		

As is reflected in Fig. 11, the temperature of water in the storage tank goes up slowly, from 23 °C to 32 °C, and the growth rate is related to hot side temperature. When T_h increases rapidly, T_w rises fast, and when T_h deceases, T_w rises smoothly.

7. Simulation

As is shown in Figs. 12 and 13, with the irradiation intensity becoming stronger, the output voltage and current of system increase fast. And the temperature of experimental room and the cold side of thermoelectric generator begins to drop, reaching their lowest point at 10:30. Then, with the difference of temperature between cold side and hot side of thermoelectric generator amplifying, the refrigeration ability of the thermoelectric devices could not keep the temperature dropping, causing the temperature of cold side to increase slowly. And what we can see from the Figs. 12 and 13 is that simulation results fit experimental data very well, revealing a maximum deviation of 0.5 °C in Fig. 12 and the average deviation 1.2 °C in Fig. 13.

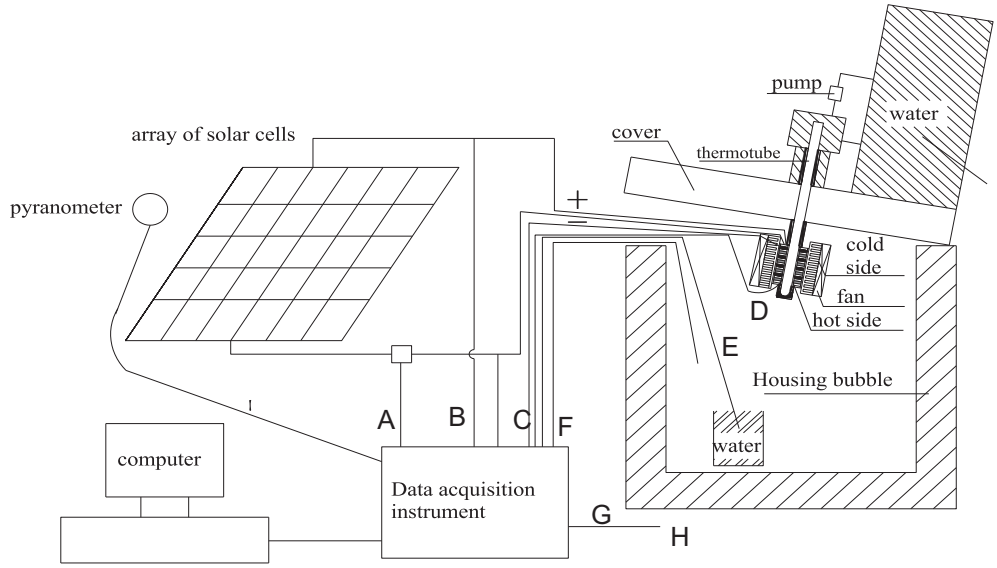

Fig. 4. The experimental set-up of the system.

Fig. 5. Actual setup of the system test rig.

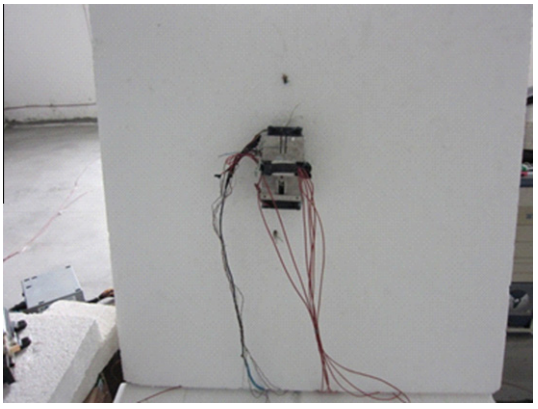

Fig. 7. Thermoelectric refrigeration component of the system.

Fig. 6. Solar cell of the system test rig.

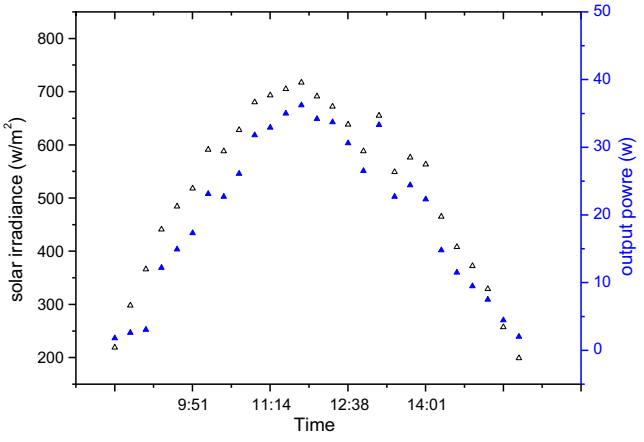

Fig. 8. Variations of output power and solar irradiance in a sunny day.

As depicted in Fig. 14, with the irradiation intensity becoming stronger, the heat released by the hot side of thermoelectric generator becomes more, leading to hot side temperature to increase and finally reach its top point at 13:00. When irradiation intensity drops, the voltage and current which the system has output decrease slowly, causing the heat release of the hot side to be cutting down. In addition, what we can see from the Fig. 14 is that simulation results and experimental data are almost the same in the morning, but deviates since noon. Maximum temperature difference occurs in the afternoon with the value about 2 °C.

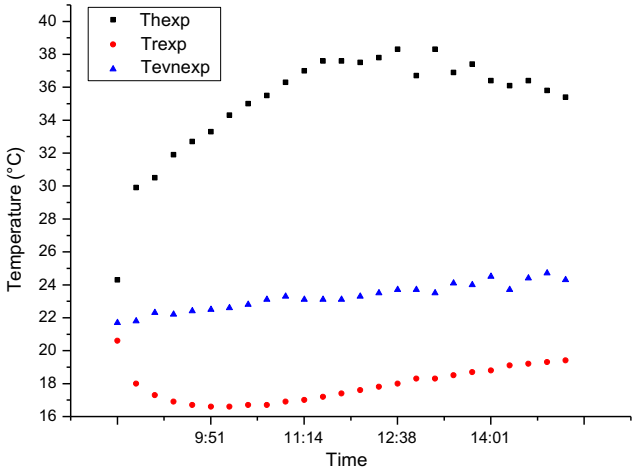

Fig. 9. Variations of T_h, T_r and ambient temperature T_{env} in a sunny day.

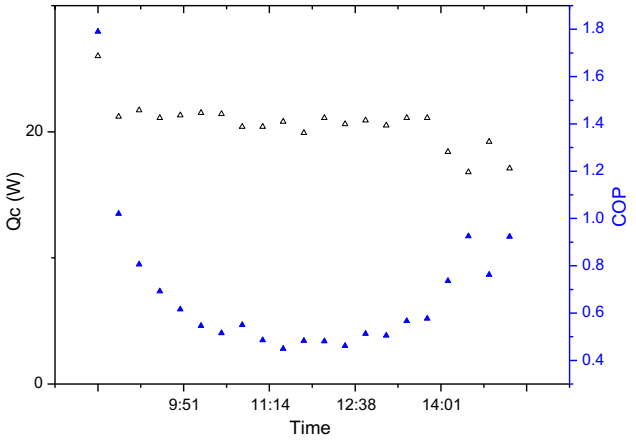

Fig. 10. Variations of COP and Q_c in a sunny day.

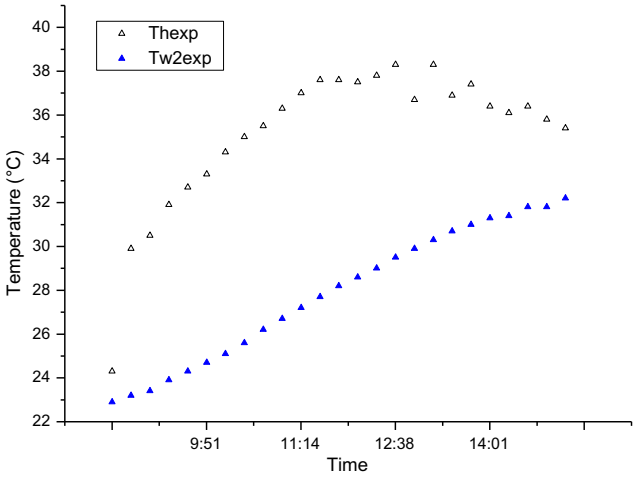

Fig. 11. Variations of T_h and T_{w2} in a sunny day.

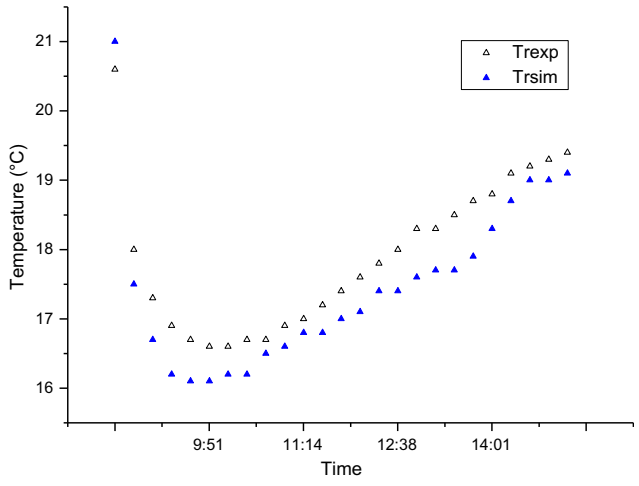

Fig. 12. The temperature of experimental room.

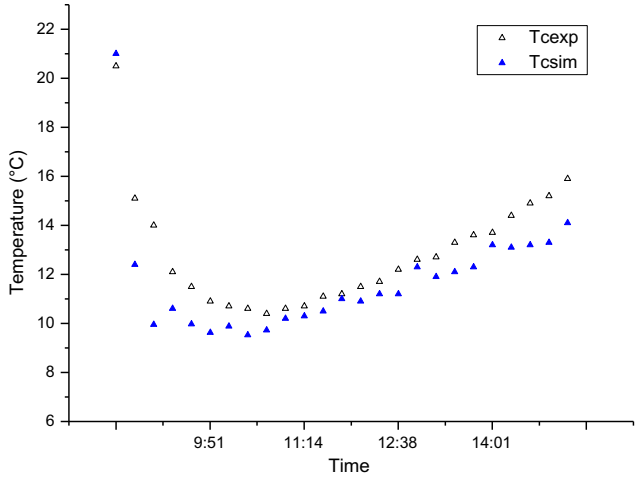

Fig. 13. The temperature of cold side.

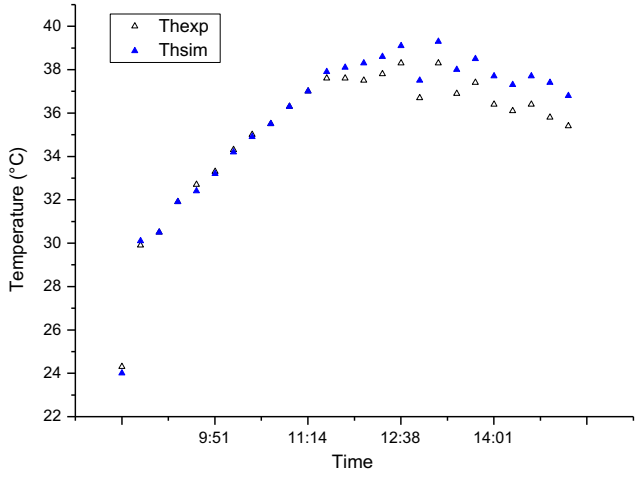

Fig. 14. The temperature of hot side.

Secondly, as is shown in Fig. 15, simulation results and experimental data of temperature in the storage tank varies similarly with that of Fig. 14. It is because that the temperature of water is related to the temperature of hot side. The temperature difference increases slowly and reaches its maximum 2 °C in the afternoon. And the thermal efficiency of this experiment is 12.06% based on Eq. (23) (see Table 2).

The average heat absorption and heat release of thermoelectric device of the system during the test.

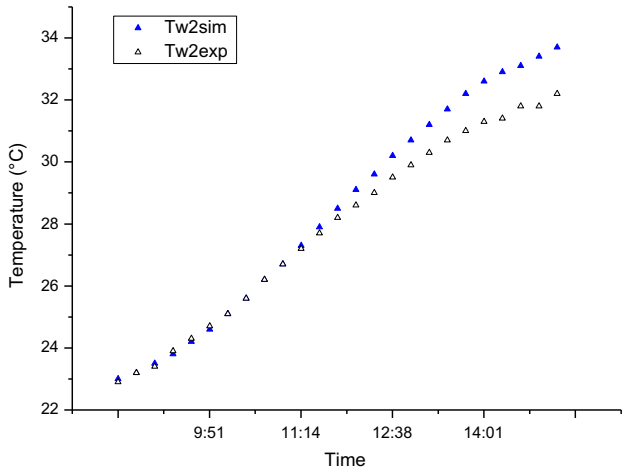

Fig. 15. The temperature of water in storage tank.

Table 2
The average heat absorption and heat gain of semiconductor chip of the system during the test.

Result	Average					
	W_{solar} (W/m^2)	Heat absorption (W)	Heat release (W)	Heat gain (J)	COP	η_t (%)
Experiment	668	20.9	59.6	41.25	0.60	12.06
Simulation		19.7	55.6	46.25	0.57	13.5

8. Conclusion

Experimental investigation on a thermoelectric cooling and heating system driven by solar has been test, and the result of the test in summer mode is presented. Comparing simulation result and experiment data, we found that they have the same trend and the system owns one excellent refrigerating capacity. But there is still difference in specific conditions, since simulations can't be exactly the same as the real phenomenon totally. Heat loss of the experimental room and the storage tank, considering with thermal resistance of various stages in the system, can affect the simulation curve. We can draw a conclusion that COP of the system is higher than 0.45, the thermal efficiency of this experiment is 12.06%, and electrical efficiency is 10.27%. In this experiment, thermal efficiency of PV/T system is not tested. If considering the thermal efficiency of PV/T system, which is reported as 41.9% [22], then there would be more thermal energy to be obtained, the thermoelectric cooling and heating system can serve family life much better.

Acknowledgements

The work described in this paper has been supported by the Program for New Century Excellent Talents in University (NCET-11-0876) and the National Nature Science Fund of China (Project No. 51078342).

References

[1] Rowe DM, Min Gao. Evaluation of thermoelectric modules for power generation. J Power Sources 1998;73:193–8.
[2] He Wei, Yuehong Su. Y.Q. Wang a, S.B. Riffat. A study on incorporation of thermoelectric modules with evacuated-tube heat-pipe solar collectors. Renewable Energy 2012;37:142–9.
[3] He Wei, Su Yuehong, Riffat SB. Parametrical analysis of the design and performance of a solar heat pipe thermoelectric generator unit. Appl Energy 2011;88:5083–9.
[4] Niu Xing, Yu Jianlin, Wang Shuzhong. Experimental study on low-temperature waste heat thermoelectric generator. J Power Sources 2009;188:621–6.
[5] Gou Xiaolong, Xiao Heng, Yang Suwen. Modeling, experimental study and optimization on low-temperature waste heat thermoelectric generator system. Appl Energy 2010;87:3131–6.
[6] Rowe DM. CRC Handbook of Thermoelectrics. 1st ed. Boca Raton: CRC Press; 1995.
[7] Chen Wei-Hsin, Liao Chen-Yeh, Hung Chen-I. A numerical study on the performance of miniature thermoelectric cooler affected by Thomson effect. Appl Energy 2012;89(1):464–73.
[8] Yamashita Osamu. Effect of interface layer on the cooling performance of a single thermoelement. Appl Energy 2011;88:3022–9.
[9] Min Gao, Rowe DM. Experimental evaluation of prototype thermoelectric domestic-refrigerators. Appl Energy 2006;83:133–52.
[10] Cheng Chin-Hsiang, Huang Shu-Yu. Development of a non-uniform-current model for predicting transient thermal behavior of thermoelectric coolers. Appl Energy 2012. online.
[11] Heremans JP, Jovovic V, Toberer ES, Saramat A, Kurosaki K, Charoenphakdee A, et al. Science 2008;321:554.
[12] Vián JG, Astrain D. Development of a thermoelectric refrigerator with two-phase thermosyphons and capillary lift. Appl Therm Eng 2009;29:1935–40.
[13] Chen Min, Lund Henrik, Rosendahl Lasse A, Condra Thomas J. Energy efficiency analysis and impact evaluation of the application of thermoelectric power cycle to today's CHP systems. Appl Energy 2010;87:1231–8.
[14] Chen Lingen, Meng Fankai, Sun Fengrui. Effect of heat transfer on the performance of thermoelectric generator-driven thermoelectric refrigerator system. Cryogenics 2012;52:58–65.
[15] Meng FK, Chen LG, Sun FR. Extreme working temperature differences for thermoelectric refrigerating and heat pumping devices driven by thermoelectric generator. J Energy Inst 2010;83(2):108–13 (6).
[16] Meng F, Chen L, Sun F. Performance prediction and irreversibility analysis of a thermoelectric refrigerator with finned heat exchanger. Acta Phys Pol, A 2011;120(3):397–406.
[17] Xia Hongxia, Luo Lingai, Fraisse Gilles. Development and applications of solar-based thermoelectric technologies. Renew Sust Energy Rev 2007;11:923–36.
[18] Dai YJ, Wang RZ, Ni L. Experimental investigation on a thermoelectric refrigerator driven by solar cells. Renew Energy 2003;28:949–59.
[19] van Sark WGJHM. Feasibility of photovoltaic – thermoelectric hybrid modules. Appl Energy 2011;88:2785–90.
[20] Hara T, Azum H. Cooling performance of solar cell driven, thermoelectric cooling prototype headgear. Appl Therm Eng 1998;18:1159–69.
[21] Atta Raghied Mohammed. Solar water condensation using thermoelectric coolers. Int J Water Resour Arid Environ 2011;1(2):142–5. ISSN 2079-7079.
[22] Pei Gang, Fu Huide, Zhang Tao, Ji Jie. A numerical and experimental study on a heat pipe PV/T system. Solar Energy 2011;85:911–21.
[23] He Wei, Zhang Yang, Ji Jie. Comparative experiment study on photovoltaic and thermal solar system under natural circulation of water. Appl Therm Eng 2011;31:3369–76.
[24] Xu Desheng. Thermoelectric refrigeration and applications. Shanghai Jiao tong University Press; 1999.
[25] Zhu YingWen, Lu XiaoDong. Thermal-resistance calculation of the forced air cooling heatsink applying for power thermoelectric devices. Power Electr 2009;6:47–51.
[26] Jie J, Hua Y, Gang P, Bin J, Wei H. Study of PV-Trombe wall assisted with DC fan. Build Environ 2007;42:1522–44.